EUROPEAN LABORATORY FOR PARTICLE PHYSICS

CERN – AB DEPARTMENT

CERN-AB-2004-009

Orbit Response Measurements at the SPS

J. Wenninger

Abstract

The optics of the SPS ring and the TT40 transfer line have been analyzed using the closed orbit (respectively trajectory) response to controlled corrector magnet deflections. A large amount of information on the machine model, beam position monitor quality and orbit corrector calibrations can be extracted from the response data. The data was analyzed with the LOCO fit program that was adapted to the SPS machine model. Data were collected on the SPS ring, and the modelling was tested in different conditions. The SPS ring data showed that a significant number of horizontal SPS orbit correctors do not provide the nominal kick strength and are damaged at the level of the magnet coil. This note describes the experience that has been gained at the SPS, the information that could be extracted from orbit data and some of the limitations of the analysis procedure in the context of the SPS.

Geneva, Switzerland

January 26, 2004

1 Introduction

A good knowledge of the linear machine model is very important in most accelerators and a number of methods exist to determine the actual optics of an accelerator. A first method consists in changing the strength of quadrupoles in a controlled way to determine the local betatron function. This *K-modulation* technique, although simple, requires individually powered magnets and a very good knowledge of the magnet transfer functions. Since most of its magnets are powered in series, this method is not adapted to the SPS. A second method determines the phase advance between adjacent beam position monitors using the betatron oscillation following a kick. This method is very powerful and is used at the SPS, but the betatron function cannot be reconstructed from the phase advance information due to the phase advance of nearly 90° between the SPS beam position monitors. Finally it is possible to extract information on the beam optics from the response of the orbit (or trajectory) to corrector magnet kicks [1]. The test of this last method at the SPS is the main subject of this document.

This note first describes a procedure to extract information on a machine model from trajectory or closed orbit analysis based on the LOCO program [1]. The analysis is then applied to data from the SPS ring. Data quality, BPM and corrector gains and tests of the program are presented. Finally the results for the short TT40 line commissioned in the fall of 2003 are also presented.

2 Orbit Response Analysis

The analysis of the machine optics in terms of orbit response is based on the relation between the beam position measured at the location of N beam position monitors (BPM) represented by a vector $\vec{u}$

$$\vec{u} = \begin{pmatrix} u_1 \\ u_2 \\ \dots \\ u_N \end{pmatrix} , \tag{1}$$

and a set of M dipole magnets (correctors) deflections (kicks) represented by a vector $\vec{\theta}$

$$\vec{\theta} = \begin{pmatrix} \theta_1 \\ \theta_2 \\ \dots \\ \theta_M \end{pmatrix} . \tag{2}$$

Orbit position and corrector deflections are related by the orbit response matrix $\mathbf{R}$ (dimension $N \times M$),

$$\vec{u} = \mathbf{R}\vec{\theta} . \tag{3}$$

Element R_{ij} of the response matrix corresponds to the orbit shift at the i^{th} monitor due to a unit kick from the j^{th} corrector. For a linear optics the matrix $\mathbf{R}$ is independent of the kick strength, respectively orbit amplitude, and the element R_{ij} is given for a closed orbit by

$$R_{ij} = \frac{\sqrt{\beta_i \beta_j}\cos(|\mu_i - \mu_j| - \pi Q)}{2\sin(\pi Q)} . \tag{4}$$

β and μ are the betatron function and phase advance, Q is the machine tune. Matrix $\mathbf{R}$ contains important information about the machine optics, albeit in a highly entangled form. On the other hand, $\mathbf{R}$ can be determined easily and in a non-destructive way.

The LOCO program [1] is a fit program that is designed to match a measured orbit response matrix of a ring or line with the machine model while properly taking into account the monitors and orbit corrector calibration errors. Orbit corrector and BPM roll angles can also be determined. LOCO has been used in various places, and the aim of this work is to test and gain experience with LOCO at the SPS for a potential future use at the LHC.

2.1 LOCO Analysis Principle

To use the information contained in the response matrix, the first step consists in building the vector $\vec{V}$ obtained by the difference between the measured and the modelled response matrix. The elements of this vector are

$$V_k = \frac{R_{ij}^{meas} - R_{ij}^{mod}}{\sigma_i} \qquad \forall i, j \tag{5}$$

where σ_i is the measurement noise of the i^{th} monitor. The norm of vector $\vec{V}$ represents the normalized error of the machine model with respect to the measurement.

The goal of the fit procedure is to minimize the norm of vector $\vec{V}$ (and therefore of the difference between model and measurement)

$$\|\vec{V}\|^2 = \sum_{k=1}^{N} V_k^2 = \text{minimum} \ , \tag{6}$$

by adjusting N_f fit parameters related to the machine model, to the monitors and to the orbit correctors. For Gaussian errors $\|\vec{V}\|^2$ should be distributed according to a χ^2-distribution. The expected minimum value for $\|\vec{V}\|^2$ is given approximately by the number of elements of $\vec{V}$ minus the number of fit parameters. The value of the minimum provides a statistical test of the fit quality and of the correct assessment of the BPM errors.

To perform a fit of the response, N_f parameters c_l must be selected, and the dependence of each element of vector $\vec{V}$ on each parameter c_l must be evaluated. The resulting sensitivity matrix $\mathbf{S}$ with elements S_{kl} defined by

$$S_{kl} = \frac{\partial V_k}{\partial c_l} \tag{7}$$

can be used to approach the solution by linearizing the problem. The three main parameter classes are :

- BPM calibration factors, where $S_{kl} = -R_{ij}^{mod}/\sigma_i$.
- Corrector calibration factors, where $S_{kl} = R_{ij}^{mod}/\sigma_i$.
- Optics model parameters (magnetic strengths, elements misalignments...). For such parameters, the sensitivity must be evaluated with a modelling program like MAD [2] using a linear approximation

$$S_{kl} = \frac{R_{ij}^{mod}(c_l + \delta c_l) - R_{ij}^{mod}(c_l)}{\delta c_l \ \sigma_i} \tag{8}$$

where the response matrix change must be evaluated for a selected increment δc_l of each parameter. Equation 8 corresponds to the local fit gradient and the increment must be chosen carefully.

The norm of vector $\vec{V}$ is minimized iteratively by solving the linear equation

$$\vec{V} + \mathbf{S}\Delta\vec{c} = 0 \tag{9}$$

for the increment $\Delta\vec{c}$ in the parameter vector $\vec{c}$. Since this equation is mathematically identical to the equation that must be solved for orbit corrections (Equation 3), it is possible to use least-square algorithms like SVD [3] and MICADO [4] to solve Equation 9. Once a new parameter vector $\vec{c} + \Delta\vec{c}$ is obtained, the procedure is iterated and the model and vector $\vec{V}$ updated. In particular, the sensitivity matrix (Equation 7) must be re-evaluated around the new optimum and Equation 9 must be solved again. This procedure is iterated until a stable solution is found, i.e. when $\Delta\vec{c} \simeq 0$.

It is important to note that matrix $\mathbf{S}$ is actually rank deficient (i.e. 'singular') : there are an infinite number of solutions obtained by multiplying both the orbit corrector strength and the orbit change by the same scale factor. For this reason it is not possible to determine the absolute calibration of orbit monitors or corrector magnets from the response matrix alone. For the horizontal plane the absolute scale can be obtained by a known energy change over the RF frequency. The radial movement can be used to calibrate the absolute scale of the horizontal monitors.

Because of the singular nature of matrix $\mathbf{S}$, Equation 9 is solved using the Singular Value Decomposition algorithm [3]. The SVD algorithm is a powerful tool to handle singular systems and to solve them in the least square sense. For a matrix $\mathbf{S}$ of dimension $n \times m$ with $n \geq m$ the singular value decomposition has the form

$$\mathbf{S} = \mathbf{U}\mathbf{W}\mathbf{V}^{\mathbf{T}} = \mathbf{U} \begin{pmatrix} w_1 & 0 & ... & 0 \\ 0 & w_2 & & \\ ... & & ... & 0 \\ 0 & ... & 0 & w_m \end{pmatrix} \mathbf{V}^{\mathbf{T}} \,, \tag{10}$$

where $\mathbf{W}$ is a diagonal $m \times m$ matrix with non-negative diagonal elements. $\mathbf{V}^{\mathbf{T}}$ is the transpose of the $m \times m$ orthogonal matrix $\mathbf{V}$,

$$\mathbf{V}\mathbf{V}^{\mathbf{T}} = \mathbf{V}^{\mathbf{T}}\mathbf{V} = \mathbf{I} \,, \tag{11}$$

while $\mathbf{U}$ is an $n \times m$ column-orthogonal matrix

$$\mathbf{U}^{\mathbf{T}}\mathbf{U} = \mathbf{I} \,. \tag{12}$$

The least-square solution to Equation 9 is

$$\Delta\vec{c} = \mathbf{V}\mathbf{W}^{-1}\mathbf{U}^{T}\ \vec{V} \tag{13}$$

where $\mathbf{W}^{-1}$ is the 'inverse' of matrix $\mathbf{W}$, with all singular elements $1/w_k > 1/\epsilon$ set to 0. $\epsilon > 0$ is a selected cut-off value that can be adapted for each data set depending in particular on input conditions (noise...).

For a machine with N BPMs and M corrector magnets *per plane*, the size of matrix $\mathbf{S}$ is

- $(2 \times N \times M) \times (2 \times (N+M) + N_f)$ if the coupling terms between the planes are ignored,
- $(4 \times N \times M) \times (2 \times (N+M) + N_f)$ if the coupling terms are included,

since the number of parameters must a priori include the calibration factors of all BPMs and correctors ($2 \times (N+M)$). The matrix size grows rapidly for large machines. For the SPS, $N \cong 120$ and $M \cong 110$, and $\mathbf{S}$ has dimensions $26'400 \times 460$. For the LHC, $N \cong 500$ and $M \cong 280$, and $\mathbf{S}$ has dimensions $\sim 280'000 \times 1'600$. While for the SPS the entire ring can still be handled by a modern desktop PC, it is essentially impossible to handle matrices of the size required for the LHC. For such a case the data can of course be split into smaller data sets by using only a subset of the orbit correctors or monitors.

3 Response Measurement and Fits at the SPS

3.1 Beam and Measurement Conditions

Orbit response measurements and tests of the LOCO fit program were performed on both fixed target and LHC MD beams at the SPS in 2002 and 2003. Measurements on the fixed target beams were performed parasitically during regular physics operation. The data was acquired in the ramp above transition, at beam energies between 50 and 80 GeV/c where the strength of the SPS orbit correctors in not yet strongly limited. The typical fixed target beam intensity was 2×10^{13} protons. Measurements on the LHC beams were mostly performed at 26 GeV/c in the MD segment of the usual fixed target cycle number 950. The typical intensity of the LHC beams was 4×10^{10} protons per bunch with up to 72 bunches per beam.

The majority of the SPS BPMs measure the beam position in one plane and they are installed next to the quadrupole providing focussing in the same plane. The orbit sampling at the SPS correspond therefore mostly to one point per cell. Since the nominal phase advance per cell is 88°, the BPM sampling limits the possibilities to identify sources of betatron beating in the machine with BPM-based measurement, both with orbit response and with phase advance measurements. This issue will be discussed in more details later.

The SPS orbit correctors are equipped with $\pm$3.5 A, $\pm$70 V power converters. The circuit time constants are typically 0.4 (0.2) s for horizontal (vertical) correctors. The magnet inductance is 4.5 (2.4) H for the horizontal (vertical) correctors. The typical ohmic resistance is in the range 10-13 Ω. The maximum available kick strength of the SPS orbit correctors at 26 GeV/c is 400 μrad for the horizontal and 210 μrad for the vertical correctors. Since the typical betatron function at both correctors and BPMs is close to 100 m in both planes, the maximum amplitudes at 26 GeV/c for a single kick are 40 mm in the horizontal and 21 mm in vertical plane. Such excursions bring the LHC beam already beyond the aperture of the ring.

For each measurement set the orbit response was recorded for a selected sample of orbit correctors. For each corrector, two orbits are recorded, for kick increments relative to the nominal setting of $\theta^+ > 0$ and $\theta^- < 0$, with $\theta^+ = -\theta^-$. For typical measurements of the linear optics, kicks corresponding to $\theta^+ \simeq 20 - 30\ \mu rad$ are sufficient. An example of raw measurement data is given in Figure 1. For each data set, the dispersion is also evaluated by recording the orbit for two different settings of the RF frequency or of the radial steering.

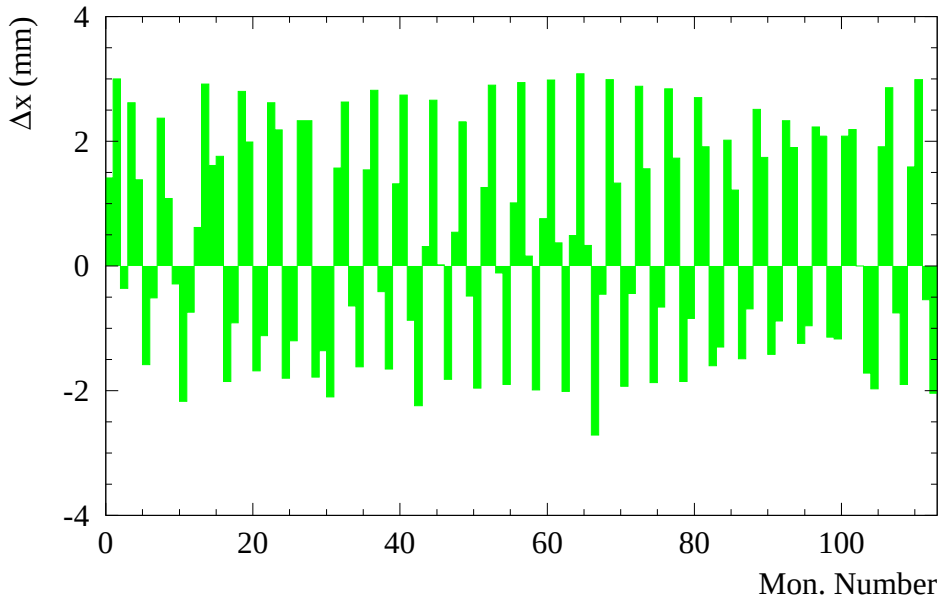

Figure 1: Example of the raw horizontal orbit response data for the SPS fixed target beam at 80 GeV/c. The data corresponds to the difference orbit ($\Delta x = x(\theta^+) - x(\theta^-)$) as a function of the BPM number. In this example $\theta^+ = -\theta^- = 30\ \mu rad$. The asymmetry of the response is due to a superimposed momentum offset introduced by the RF radial loop (see Section 3.2.2).

3.1.1 Beam Position Monitor Noise

The typical BPM measurement noise, obtained by recording a number of orbits at constant orbit corrector setting and recording the r.m.s. position change at each BPM during a typical measurement, is shown in Figure 2 for the fixed target and LHC beams. This definition of the BPM noise obviously includes the intrinsic electronic noise and the beam stability in the SPS. The r.m.s. noise of each individual BPM is used in Equation 5 as weight factor for the difference between data and model. Figure 2 shows that the noise is significantly lower for the fixed target beam, which may be a consequence of the different acquisition modes used for the two beams. Depending on beam and machine conditions (intensity...) the r.m.s. noise can be up to 50% larger than the values indicated in Figure 2. It is important to note that a non-linear response of the BPMs may introduce additional 'noise' that is not included in the noise estimate based on the orbit stability.

3.2 SPS Fit Parameters

3.2.1 Gain Factor for Monitors and Corrector Magnets

Since in general neither the monitor nor the orbit corrector calibration factors are known precisely, they must included in the free parameters of the fit. This corresponds to 113 monitor calibration factors for each plane, plus the calibration factors of the correctors that are used for a given measurement. In general only a sub-sample of $n_c \simeq 20 - 60$ of the 108 orbit correctors

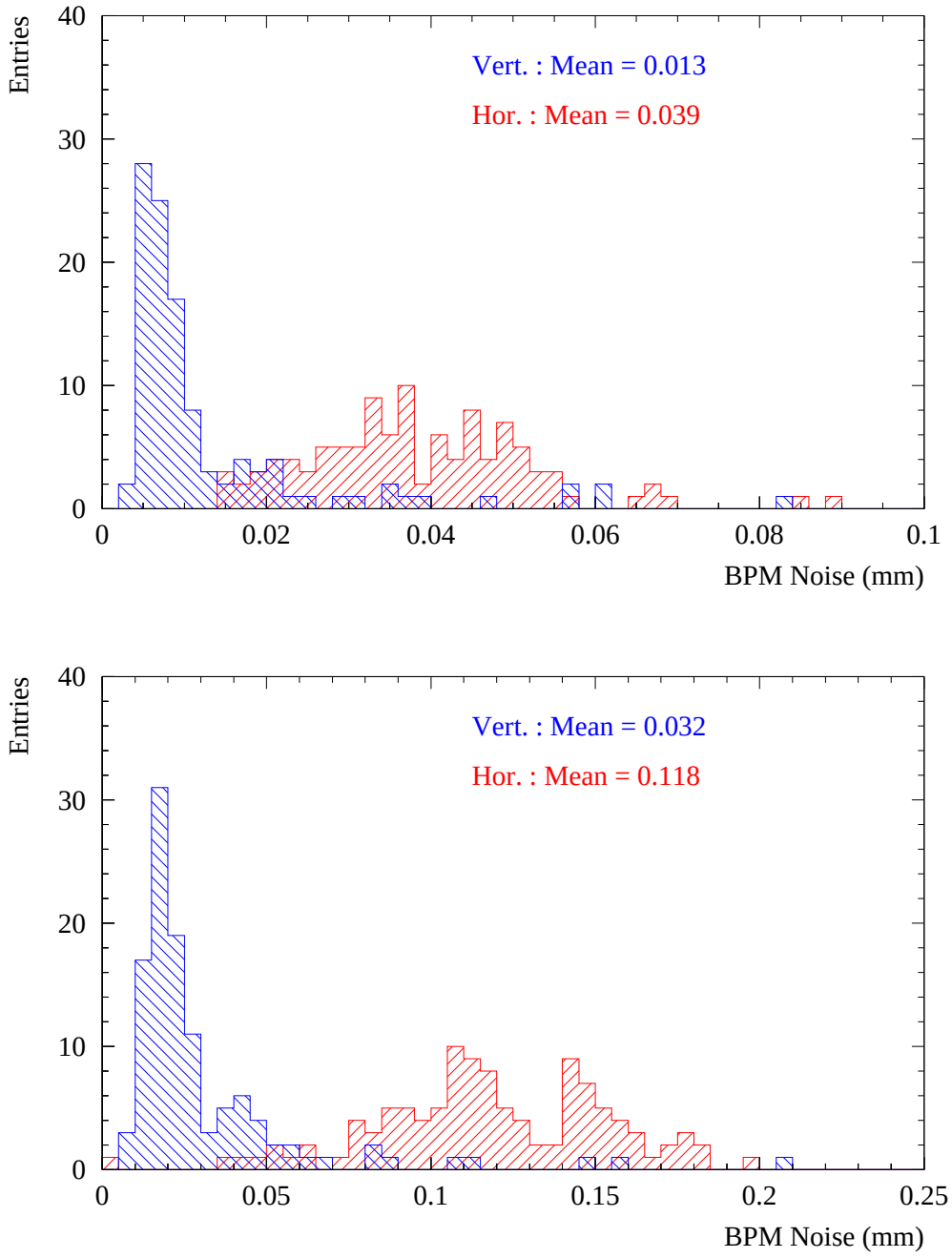

Figure 2: Typical noise / orbit reproducibility distribution at the BPMs for a fixed target beam (top) and for a LHC MD beam (bottom). There is one entry in each histogram per BPM.

available in each plane is used. The calibration factors are defined as

$$u_i^{fit} = C_i \; u_i^{meas} \tag{14}$$

where u_i^{meas} is the measured BPM response or the nominal corrector strength and C_i is the calibration factor. In most of the figures presented in the following sections, the measured response is automatically corrected for the calibration factors.

3.2.2 Momentum Offsets

An independent momentum offset is determined for each corrector response to take into account fluctuations or systematic shifts of the momentum offset δ. The measured dispersion is used in the fit to adjust the momentum offset. This fit parameter is important for two reasons.

First, the radial position of the SPS fixed target beam is controlled by a radial loop that uses the signal of the BPM BPCR.31202 in sextant 3. When the beam position is changed for the response measurements, a position shift at the BPCR results in a momentum shift introduced by the radial loop to maintain the beam position at BPCR at its reference value. The momentum shift δ^j for a kick θ_j the jth corrector is given by

$$\delta^j = -\frac{\sqrt{\beta_x^{rad}\beta_x^j}}{2\sin(\pi Q_x) D_x^{rad}} \; \cos(|\mu_x^{rad} - \mu_x^j| - \pi Q)\, \theta_j \tag{15}$$

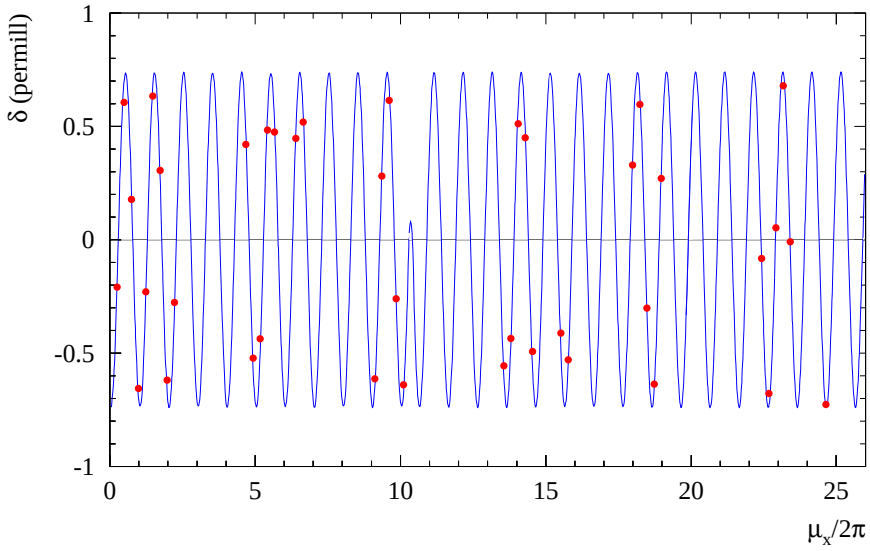

Figure 3: Reconstructed momentum shift δ as a function of the horizontal phase advance μ_x due to the beam position change at the radial RF BPM for a number of horizontal orbit correctors (•). The solid line is the expected shift as a function of the corrector phase advance at a β-function of 100 m.

where the label rad refers to the radial BPM, D_x is the horizontal dispersion. The reconstructed shifts are compared to the expected shift for a number of horizontal orbit correctors in Figure 3. The agreement between the expected momentum change and the measurements is excellent.

Secondly, for the LHC beam where the RF frequency is held constant, the corrector kick induces an orbit lengthening ΔL_1^j given by

$$\Delta L_1^j = D_x^j \theta_j \tag{16}$$

Since the RF frequency is fixed, the beam must adapt its radial position which produces a relative momentum change

$$\delta^j = \left(\frac{1}{1/\gamma^2 - \alpha_c} \right) \frac{\Delta L_1^j}{C} \tag{17}$$

α_c is the momentum compaction factor, γ is the relativistic factor and C the machine circumference. For large deflections relative momentum changes of $\sim 10^{-4}$ are easily produced.

3.2.3 Optics Strength Parameters

The standard MAD SPS model was used for most of the response data fits. In general 6 independent strength parameters were adjusted with LOCO. They correspond to the strength of the vertical focusing quadrupole chain KQD covering the entire SPS and to the 2 horizontally focusing quadrupole chains KQF1 and KQF2 that split the SPS ring into two halves. This additional degree of freedom for the horizontal tune is used to adjust the phase advance between the West and North electrostatic septa for the slow extracted fixed target beam while maintaining the machine tune at a fixed value. Three additional degrees of freedom, KQF1A (2 quadrupoles), KQF2A (5 quadrupoles) and KQDA (8 quadrupoles) correspond to the strength of the enlarged quadrupoles (QMA) associated to each of the main quadrupole chains. It must be noted that in practice the enlarged quadrupoles share the same converters than the normal aperture magnets : they cannot be set independently of the normal quadrupoles. Their strength was used as fit variable to verify that the relative strength of normal and enlarged quadrupoles corresponds to the expected value. A fit based on those 6 parameters essentially adjusts :

- the machine tunes,
- the sharing of the horizontal phase advance among the two halves of the SPS ring powered by the QF1 and QF2 quadrupole chains,
- possible strength errors due to the difference between the normal (QM) and enlarged aperture (QMA) quadrupoles.

Figure 4 shows a typical measured and fitted orbit response with the SPS fixed target beam for a deflection θ^+ of 0.03 mrad, while Figure 5 shows the corresponding data with the LHC beam for a horizontal excursion that brings the beam close to the edge of the available horizontal aperture. The data shown in the figures correspond to the difference between the response for θ^+ and θ^-. One notes the excellent agreement between data and model after the fit, performed with the 6 strength parameters described above. The residual differences that are also shown in the figures correspond to only $\sim$ 2% of the response, indicating the very good agreement between the SPS model and the actual machine. One can however note that the residuals are significantly above the noise level (Figure 2) and are not entirely random, but show patterns that indicate a

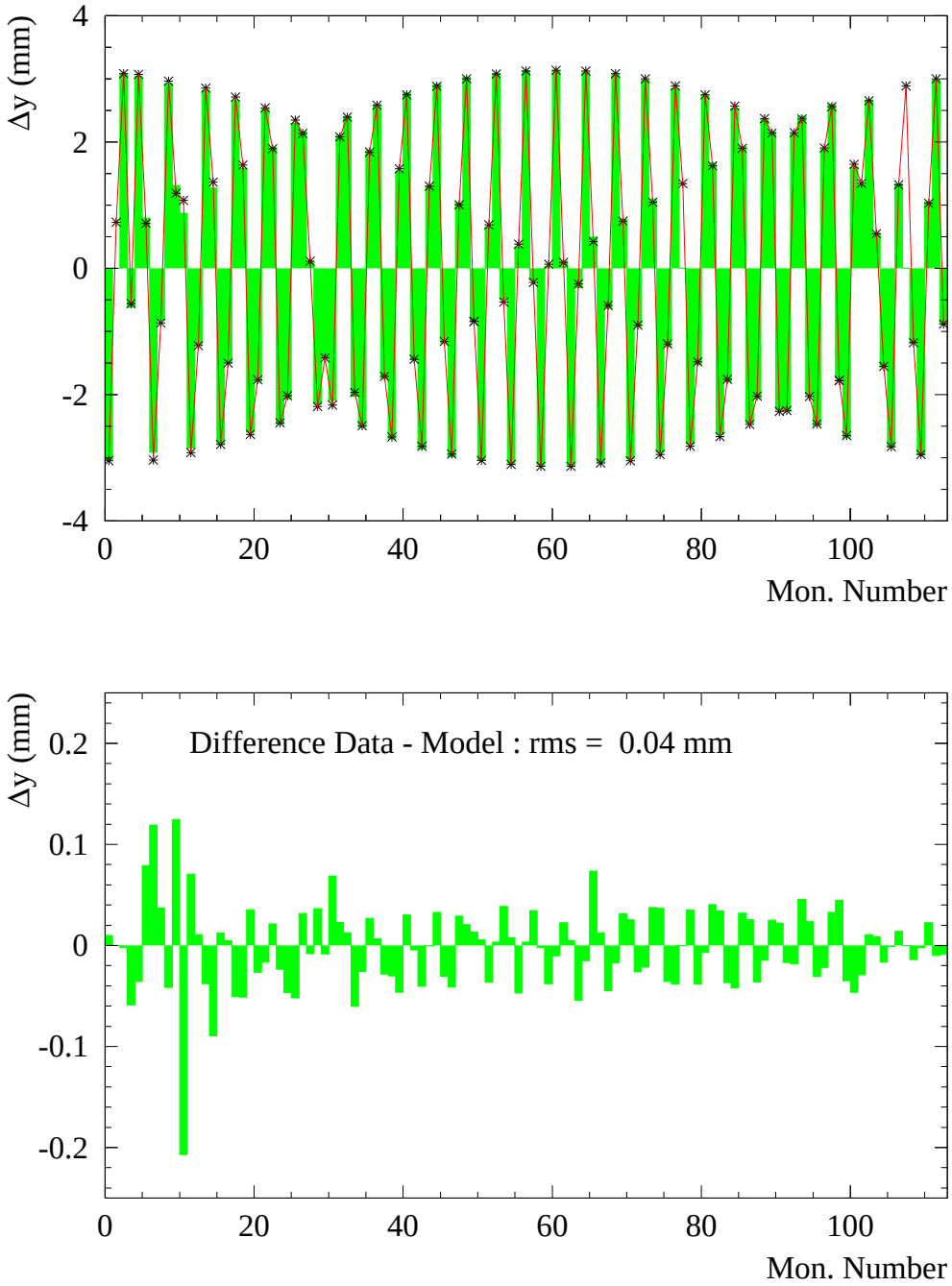

Figure 4: Top : vertical orbit response ($\Delta y = y(\theta^+) - y(\theta^-)$) at 80 GeV/c for $\theta^+ = -\theta^-$ = 0.03 mrad at vertical orbit corrector MDV.107 in the SPS ring. The horizontal axis indicates the BPM number. The histogram represents the measured response corrected for BPM calibration factors, while the symbol * corresponds to the fit model. Bottom : difference between data and model for the same orbit response.

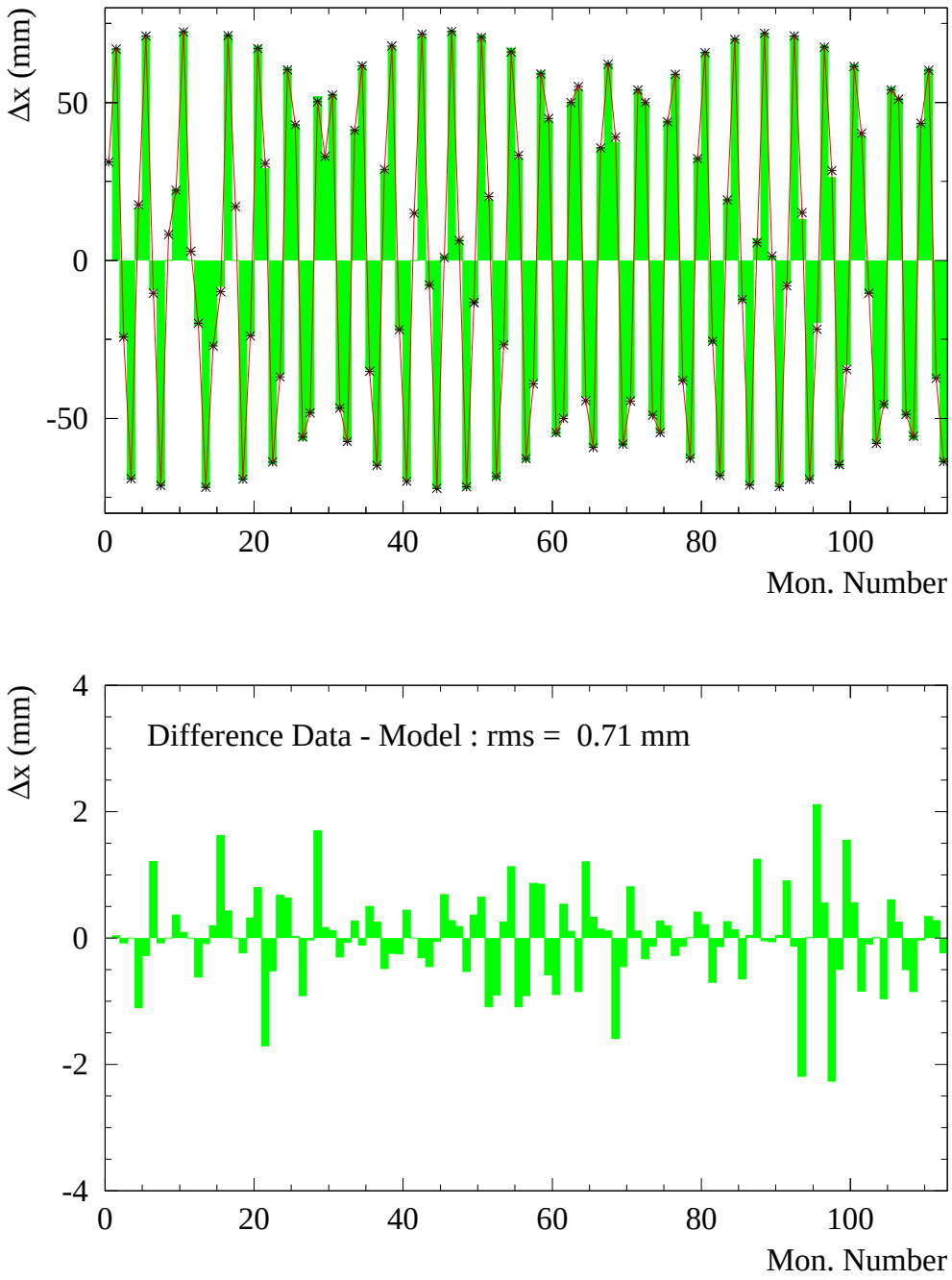

Figure 5: Top : horizontal orbit response ($\Delta x = x(\theta^+) - x(\theta^-)$) at 26 GeV/c for $\theta^+ = -\theta^-$ = 0.35 mrad at horizontal orbit corrector MDH.420 in the SPS. The horizontal axis indicates the BPM number. The green histogram represents the measured response corrected for BPM calibration factors, while the * correspond to the fit model. For this example the LHC beam was bumped close to the available horizontal aperture of the ring for $\varepsilon^* \simeq 3.5$ μm. Bottom : difference between data and model for the same orbit response.

residual model error. The strength differences between normal and enlarged quadrupoles that are predicted by the fits are generally very small, at the level of a few permill. The resulting change of the β-function is at the level of 1-2%.

For the data sample corresponding to the example shown in Figure 5, a special SPS model including field errors of the main dipoles (mainly sextupole errors) and main quadrupoles (octupole errors) was also used for the fits since the orbit excursion are very large [6]. A marginal improvement of the fit is obtained, but the BPM noise and is not sufficient to resolve correctly the effect of non-linear fields even for the largest orbit excursions due to their very small contributions.

Attempts to improve the agreement between data and model by performing a fit where all 216 SPS quadrupole strengths were allowed to vary freely result in better agreement between data and model. But the horizontal dispersion predicted by such fits is in general in very poor agreement with the measured dispersion, indicating that the fit improvement is artificial : the fit gives a better match with the orbit response but the resulting model does not correspond to the actual SPS machine, possibly because some of the fit improvements actually compensate measurement errors of the BPMs rather than true optics errors.

All fits to SPS data using the 6 global strength described in the beginning of this section result in some residual difference between data and model that corresponds to 1-3% of the orbit response. The difference can be above the noise level and exhibits distinct patterns that are not due to random noise. Such differences may indicate an un-modelled betatron beating of $\sim 10\%$, in agreement with the phase advance beating observed between adjacent BPMs obtained from multi-turn acquisitions. A non-linear response of the SPS BPMs may also explain part of the difference data-model. The strength differences between normal and enlarged quadrupoles that

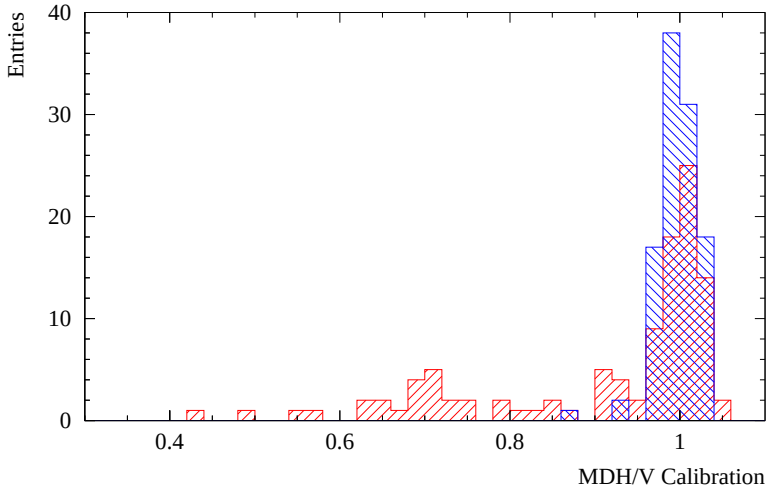

Figure 6: Distribution of the orbit corrector gain calibration factors for the horizontal (red) and vertical plane (blue). The horizontal gain factors exhibit a long tail extending down to gains of 0.4. Simulations shown that the accuracy of the calibration factors is in the range of 0.2 to 0.6% depending on the BPM noise.

are predicted by the fits are generally very small, at the level of a few permill. Simple fits based on the nominal strength ratio between normal and enlarged quadrupoles yield only very slightly worse fits.

3.3 Gain Calibration Results

3.3.1 Orbit Corrector Calibration

The analysis of the orbit corrector kicks in the SPS soon revealed unexpectedly small kicks for a number of horizontal orbit correctors [5]. The distribution of horizontal gain factors for the orbit correctors exhibits a long tail extending down to 0.4 as shown in Figure 6. No such effect is observed for the vertical orbit correctors. The distribution of the scale factors as a function of the longitudinal position in the SPS ring is not entirely homogenous, see Figure 7, but the weak correctors do not seem to cluster in a special location. Various tests with nominally closed 3 corrector bumps confirmed the missing kick strength of the horizontal orbit correctors. A circuit analysis by the PO-group indicated an abnormal frequency dependence of the transfer functions for the weak correctors. A selected sample of the weakest orbit correctors, MDV.11107, MDV.30207, MDV.40607, MDV.50207 and MDV.50807 were replaced in the winter shutdown 2002-2003. After replacement with new magnets, the orbit correctors now provide the nominal kick strength, thus confirming that the coils of the weak horizontal orbit correctors are damaged by inter-turn short circuits. The reason why the damage does not affect the vertical orbit correctors is not understood, but it might be due to radiation damage from proton losses or synchrotron light that mainly affects coils positioned in the horizontal plane, as is the case for the horizontal orbit correctors but not for the vertical correctors.

3.3.2 Beam Position Monitor Calibration

The calibration factors of the BPMs exhibit a typical RMS spread of 4 to 5% around the mean value, as shown in Figure 8. The calibration factors are reproducible for a given beam to $\sim$ 1-2%, even from one run to the next, at least for the large majority of the BPMs. The simulated accuracy of the calibration factors ranges from 0.5 to 1.5% depending on the noise and the number of orbit correctors used for the LOCO fit. Since the absolute scale of BPMs and correctors magnets cannot be determined from the orbit response alone, the scale of the BPM gain factors has been defined assuming that the corrector magnet calibration factor (and therefore deflection) is correct. The horizontal scale is only defined by the corrector magnets with a calibration factor near 1 in Figure 6. With this assumption the average BPM scales must be corrected by a factor 1.09 ± 0.01 for the horizontal and 0.95 ± 0.01 for the vertical plane.

The absolute horizontal BPM scale can be obtained independently from a change of the radial position, provided the RF frequency is recorded at the same time. Such a measurement was performed at 450 GeV/c on the LHC beam. The RF frequency was changed around its central value, with a total frequency difference between two orbits of 701 ± 2 Hz. From the momentum compaction factor of the SPS, $\alpha_c = 1.92 \times 10^{-3}$ corresponding to the LHC beam tunes of $Q = (26.18, 26.13)$, it is possible to evaluate the momentum change and to reconstruct the horizontal dispersion from two associated closed orbits. Figure 9 compares the expected dispersion function obtained from the measured RF frequency with the model. The measured dispersion must be scaled by a factor 1.18 to match the model, compared to the factor 1.09

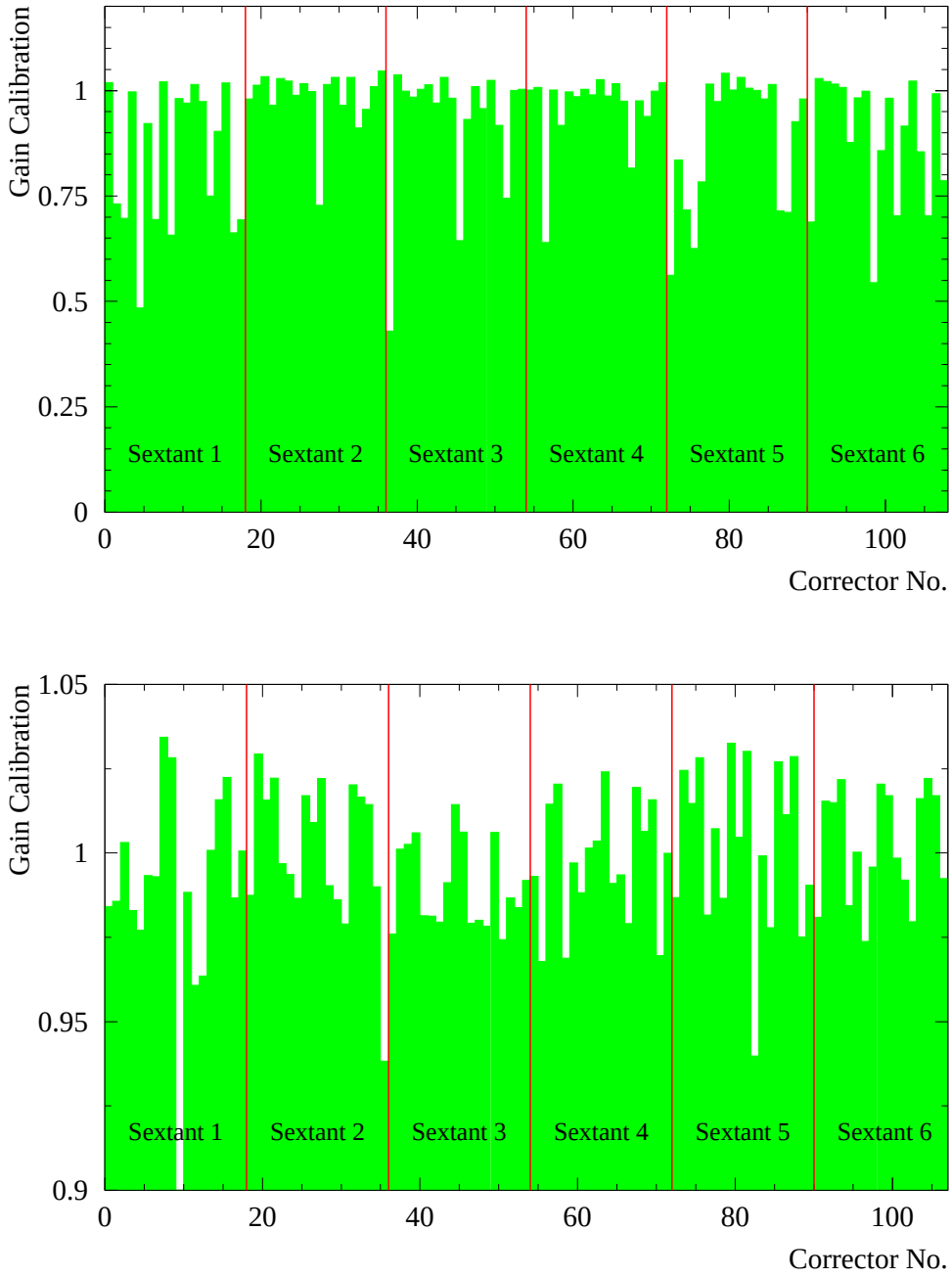

Figure 7: Orbit corrector gain calibration factor as a function of the longitudinal position along the SPS ring for the horizontal (top) and vertical correctors (bottom). Note the difference in the vertical scale between horizontal and vertical orbit correctors.

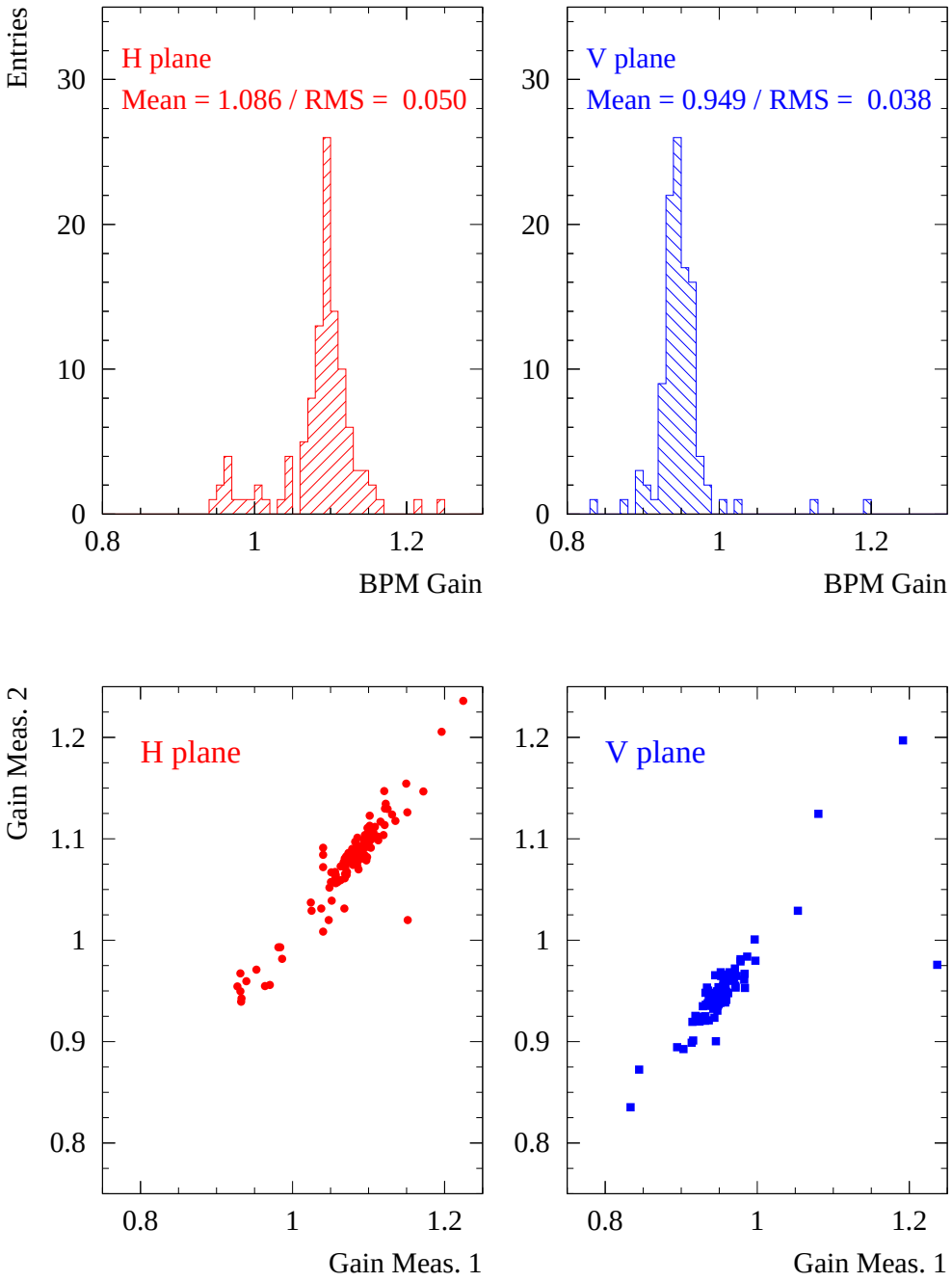

Figure 8: Typical distribution of the BPM calibration factors for the fixed target or LHC beams (top). The scale of the BPM gains is defined with the assumption that the corrector magnet deflections are on average at the nominal strength. The correlation of calibration factors obtained from two measurement sets separated by 5 days is shown below. There is a good correlation, and the gains are reproducible to within 1%.

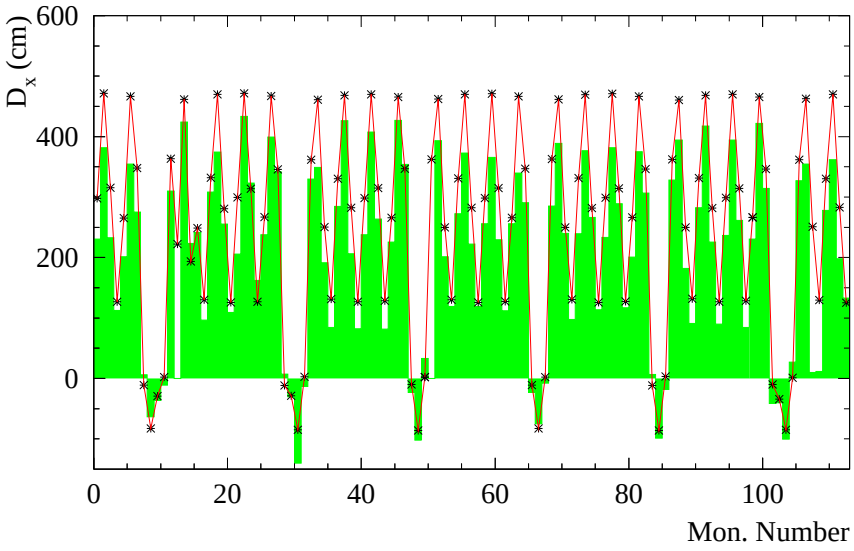

Figure 9: Comparison the the expected and reconstructed horizontal dispersion in the SPS at 450 GeV/c for a controlled change of the RF frequency. The uncorrected measurements do not agree with the model, indicating a 18% scale error on the BPM gains.

obtained at lower energies from the orbit response measurements. The difference may be explained by a scale error of 9% of the horizontal corrector kicks. The BPM scale error may be related to the impedance adapters installed on the BPMs. The adapters may have aged because they were never changed since the construction of the SPS. The adapters are not included in any of the calibration procedures of the BPMs.

For the vertical plane an independent verification of the absolute scale was obtained at 26 GeV/c using the beam-beam compensator BBLR.517, a wire installed in the SPS as a vertical distance of $\sim$ 20 mm from the beam axis to simulate long range beam-beam effect in the SPS. The tune changes observed when the wire is powered and the beam dumped towards the wire confirm that the BPM and corrector calibration scales are correct within a few percent.

3.4 Optics Tests of LOCO

The possibility to identify local optics errors due to quadrupole errors was tested with the LHC beam at 26 GeV/c using some of the few individually powered quadrupoles in the SPS.

The orbit response was measured first under standard machine conditions. Then the individually powered quadrupoles QE603 (located at a position with large vertical β-function) and QE604 (located at a position with large horizontal β-function), that are switched off for normal operation, were powered at -14 A (QE603) and +12 A (QE604) for two different measurement sets. The strength changes that are expected from the magnet calibration tables are $K_{QE603} = -6.3 \cdot 10^{-2}$ (m^{-2}) and $K_{QE604} = +5.4 \cdot 10^{-3}$ (m^{-2}). In both cases the machine tunes were corrected back to the reference values. The expected β-beating is $\sim$ 25% in the horizontal plane and $\sim$ 5-10% in the vertical plane for QE604, while for QE603 the effects are reversed between horizontal and vertical plane.

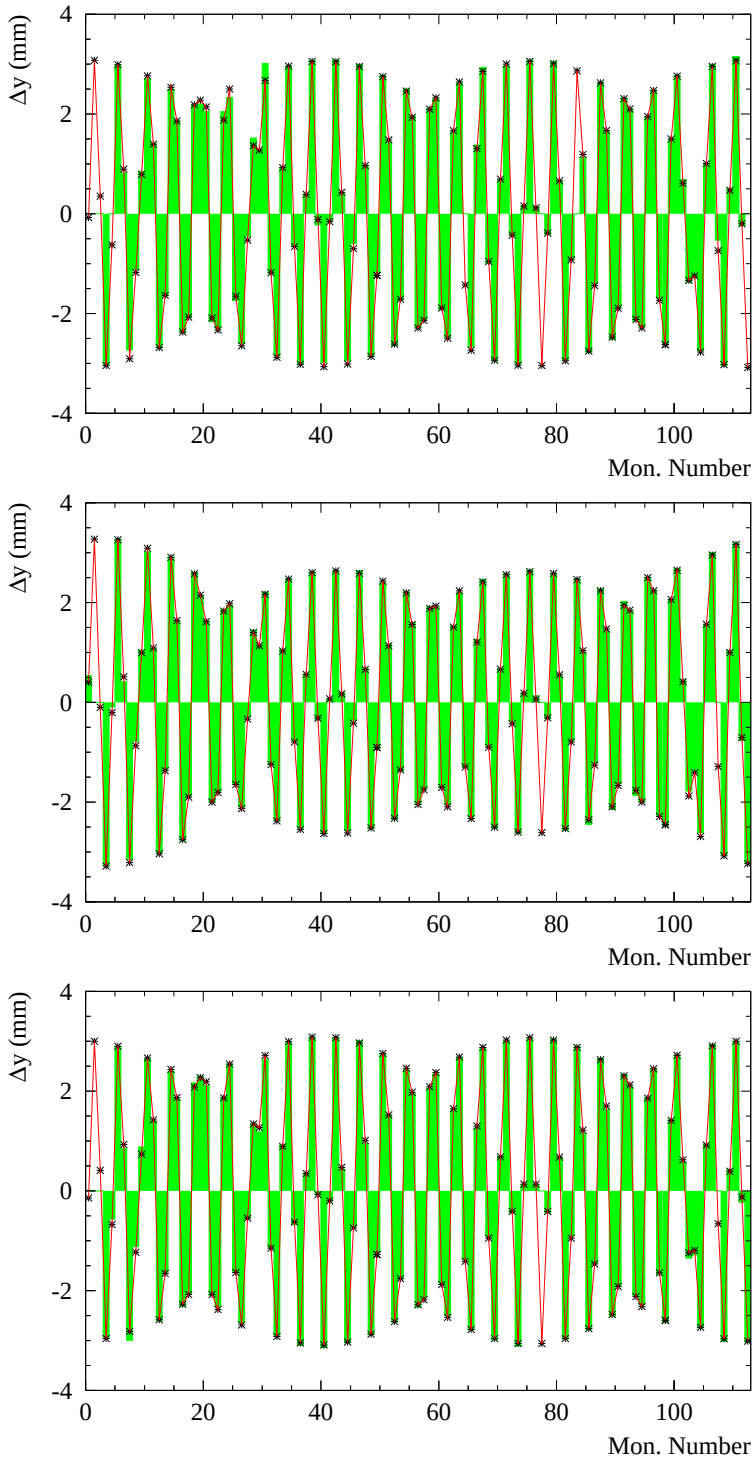

Figure 10: Measured (histogram) and fitted response (*) of vertical corrector MDV.201 for the nominal optics (top), for the optics distorted by quadrupole QE603 (middle) and a similar perturbation due to quadrupole QE604 (bottom). In all cases fit model and data agree very well. As expected the effect of QE603 is more significant for this corrector since it is located at a place of large β_y.

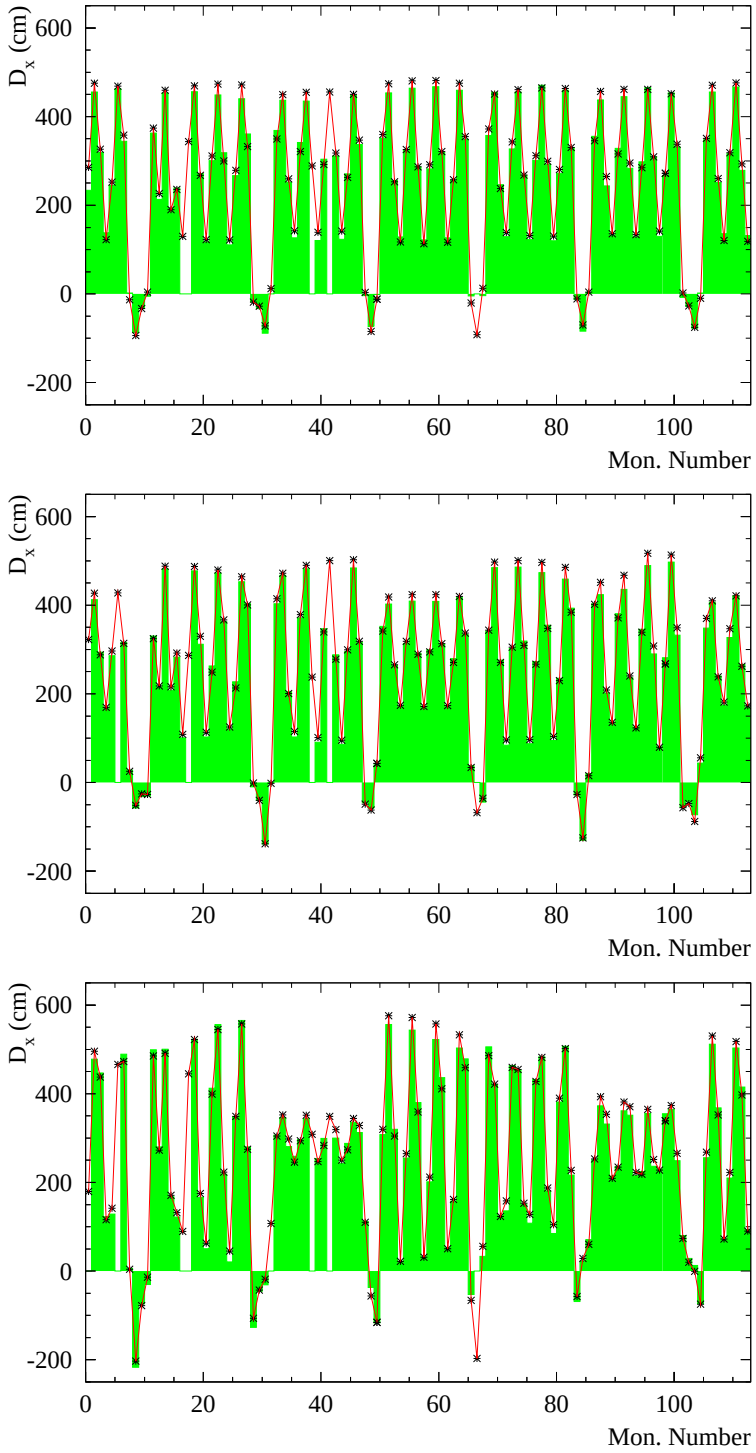

Figure 11: Measured (histogram) and fitted dispersion (*) for the nominal optics (top), for the optics distorted by quadrupole QE603 (middle) and a similar perturbation due to quadrupole QE604 (bottom). In all cases the model fits the data rather well, with an r.m.s. difference of model and data of $\sim$ 10 cm.

Data set	K_{fit} (10^{-3} m^{-2})			
	QE603	QE604	QE605	QE606
All QE off	-0.25	0.59	0.19	-0.37
QE604 : $I = +12$ (A), $K = +5.4 \cdot 10^{-3}$ (m^{-2})	-0.33	5.94	0.18	-0.47
QE603 : $I = -14$ (A), $K = -6.3 \cdot 10^{-3}$ (m^{-2})	-6.71	0.03	0.12	-0.76

Table 1: Fit results for the strengths of the 4 QE quadrupoles for the 2 measurement sets and for a reference situation with both QE quadrupoles switched off. The fitted strength changes agree with the expected changes. The typical fit error can be estimated to $\sigma_K \simeq 0.3$ (10^{-3} m^{-2}) from the results for the QE605 and QE606 strengths.

The fits of the SPS model were performed for all 3 data sets with the 6 strengths KQD, KQDA, KQF1, KQF1A, KQF2 and KQF2A that were described previously and with 4 additional individual strengths for quadrupoles QE603, QE604, QE605, and QE606 for a total of 10 free optics parameters. Figure 10 compares the measured and modelled response of one vertical orbit corrector and Table 1 gives the LOCO fit results for the QE quadrupole strengths. LOCO is clearly able to identify the correct quadrupole, and the strengths are in good agreement with the values expected from the magnet calibration curves. The uncertainties on the strengths correspond roughly to $\sigma_K \simeq 3 \times 10^{-4}$ m^{-2}. Including 8 additional individual quadrupole strengths distributed over the SPS ring does not change the fit result significantly : in each case LOCO is able to identify correctly the source of the optics error.

A powerful cross check of the fit results is obtained from the horizontal dispersion, since this parameter is not directly part of the LOCO fit. Figure 11 shows the horizontal dispersion data and model for the nominal and the perturbed optics. A very good agreement is obtained from the fit model and the measurement when the QE quadrupoles are powered, thus providing a nice cross-check of the good fit quality.

3.5 Fit Biases

Although the optics test described in the previous section was successful, the phase advance of almost exactly 90° between adjacent BPMs is rather unfavorable for the measurement and analysis of optics errors since the phase advance of the β-function beating is nearly 180° between nearby BPMs.

An additional problem may arise if the fit parameter set is not adequate, i.e. when the source of the optics errors does not match the available free parameters of the fit. To illustrate this point we consider the example of a single localized strength error of $\Delta K = 3.5 \cdot 10^{-3}$ (m^{-2}) at quadrupole QF1.410 in the SPS. The corresponding β-function beating amplitude is 25% in the horizontal and 10% in the vertical plane. Provided the measurement noise is adequate and the strength of the corresponding quadrupole is available to LOCO as free parameter, the fit program is able to identify the source of the beating efficiently, as demonstrated in the previous section. The situation changes if the only available free parameters are the main quadrupole strengths KQD, KQF1 and KQF2. Since the quadrupole responsible for the optics error is not available for the fit, the LOCO program will adjust all other parameters and try to 'absorb' the betatron beating. Figure 12 illustrates the effect of such a fit on the BPM and orbit corrector gain factors : the local β-beating has been partly absorbed in the BPM and corrector calibration

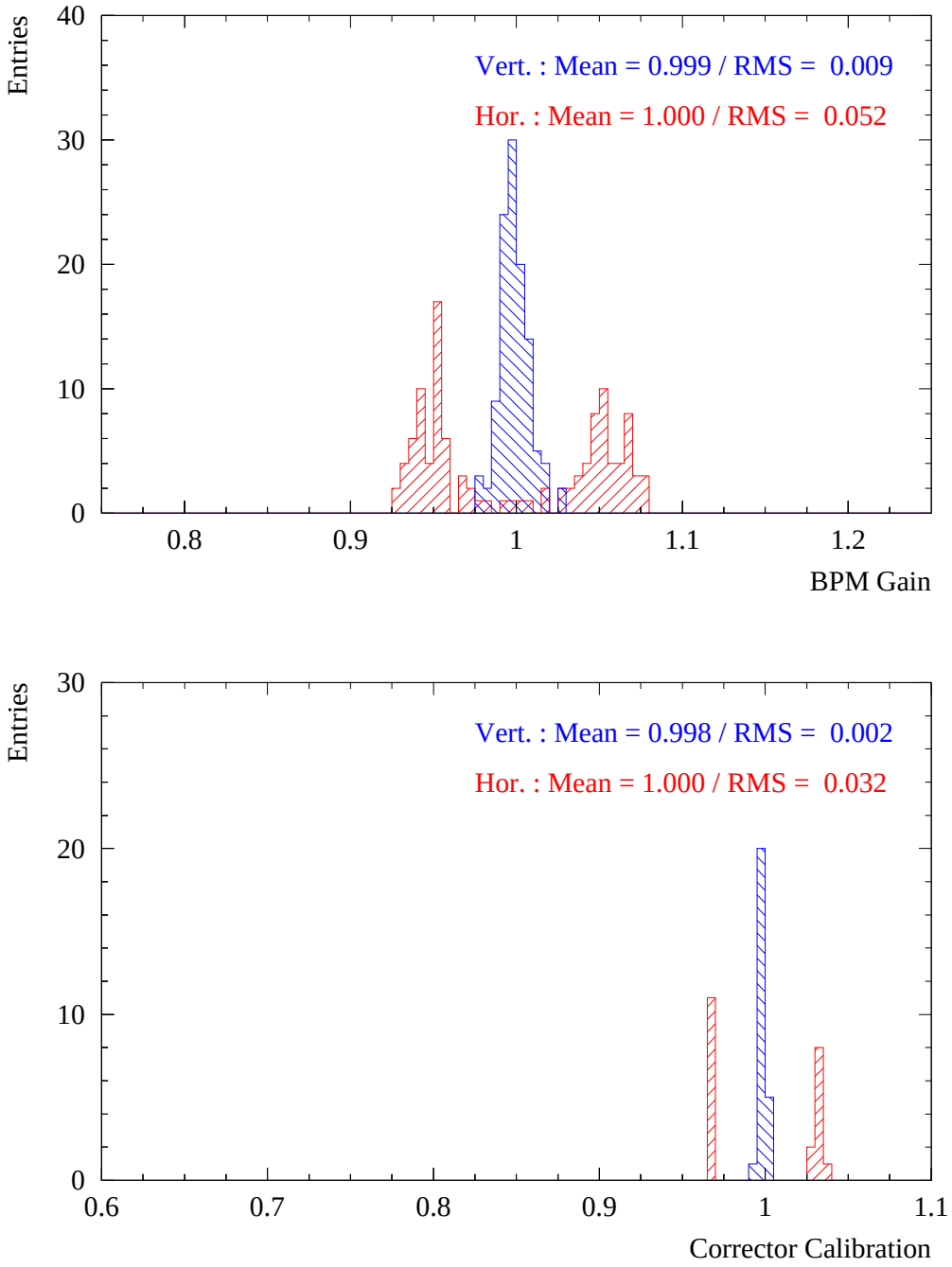

Figure 12: BPM (top) and orbit corrector (bottom) calibrations obtained from a fit simulation for a 25% horizontal and 10% vertical betatron beating induced by a localized strength error due to a single quadrupole. Part of the betatron beating has been absorbed by the fit into the calibration factors of BPMs and correctors. For this simulation all BPM and corrector gains are perfect and the BPM noise is negligible.

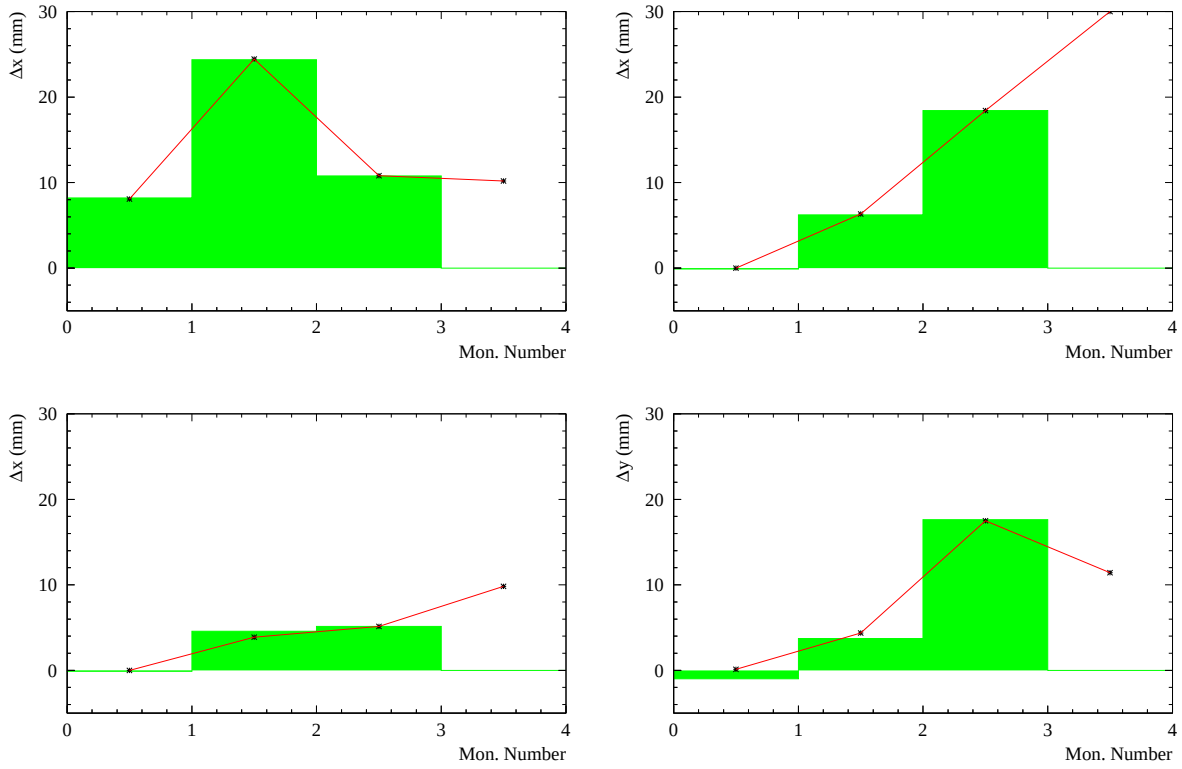

Figure 13: Measured (histogram) and fitted (*) trajectory response for the TT40 transfer line of the SPS. There is no data for the 4^{th} monitor that is installed behind the TT40 TED beam dump. The data corresponds to the magnetic septum MSE.418 (top left, $\Delta\theta = \theta^{+} - \theta^{-} \simeq 70\ \mu rad$), to the MBHC.4001 dipole (top right, $\Delta\theta \simeq 165\ \mu rad$), to the horizontal corrector magnet MDMH.4001 (bottom left, $\Delta\theta \simeq 175\ \mu rad$) and to the vertical corrector magnet MDMV.4000 (bottom right, $\Delta\theta \simeq 175\ \mu rad$).

factors that exhibit double peaks corresponding to the betatron beating. Despite the bias of the calibration factors, the fit residual between data and model never agree within BPM noise that is typical for the SPS.

The consequence of betatron beating on fit quality and on gain bias depends on the exact errors and on the available fit parameters. From the present example and the observed r.m.s. spread and shape of both corrector and BPM calibration distributions, see Figures 6 and 8, it is possible that a few percent betatron function beating may be 'hidden' in the SPS ring data presented in the previous section. This estimate is in agreement with phase advance measurements. It is also consistent with the difference between the measured and the modelled horizontal dispersion.

4 The TT40 Transfer Line to CNGS and LHC

The fast extraction channel in LSS4 and the TT40 transfer line from the SPS to the CNGS target and LHC ring 2 have been commissioned in September and October 2003. During the

two 24 hour beam extraction tests, the 100 m long TT40 line optics was verified by measuring the trajectory response of the few available steering elements.

The trajectory measurements were performed with pilot bunches of 5×10^9 protons for which the BPM resolution is limited to 0.2 mm by measurement noise. The kick ranges $\Delta\theta = \theta^+ - \theta^-$ were in the range of 70 to 175 μrad. The fit results are shown in Figure 13 for all 4 steering elements : the magnetic septum MSE.418, the main dipole string MBHC.4001 and the first horizontal and vertical corrector magnets. For the fit shown in Figure 13 only the BPM and steerer calibration factors were adjusted. The fitted deflections agree within $\sim$ 5% with the expected values, except for the septum kick that is found to be 20% lower than expected. This reduction may be due to hysteresis effects. The third horizontal BPM signal was found to have the wrong sign (corrected in Figure 13), but all other BPM gain factors were consistent with 1 within $\sim$ 15%.

The number independent measurements being very small, it is not possible to perform a fit for all gains and the two TT40 quadrupole strengths at the same time. Only a single quadrupole strength can be allowed to vary for a given fit. The fit was therefore repeated once with each of the two quadrupole strength as additional free parameter. The results yield strengths that agree within 10% with the nominal strengths. The deviations are consistent with errors expected from the BPM resolution.

5 Conclusion

The LOCO program was successfully tested experimentally for the SPS ring and the TT40 extraction line. The aim of this programs is to adjust the machine model to measured orbit or trajectory responses. Furthermore it has the ability to fit both BPM and orbit corrector calibration factors.

The main outcome of the measurements at the SPS are :

- The orbit response analysis confirmed the good agreement between model and machine for the linear optics. Unexplained differences correspond to a few percent of the orbit response and may be explained by a few percent β-beating.
- A significant number of horizontal SPS orbit correctors were found to the damaged by inter-turn short-circuits. No such effect was seen for the vertical orbit correctors.
- The ability of the LOCO program to adjust the machine model was tested by varying the strengths of individually powered quadrupoles. The fitted model strengths agree well with the expected set values, indicating that it is possible to tune the machine model with orbit response data.
- To obtain meaningful results it is not always sufficient to provide the fit program with a large number of optics strength parameters. Although the fit quality tends to improve thanks to the large number of free parameters, a cross-check of the model through the dispersion often indicates that the resulting model does not describe the horizontal dispersion and that the model was biased by measurement errors.

The measurements that have been discussed in this document refer all to the SPS optics at low momentum, mainly because the available kick strength is strongly limited at the 450 GeV/c LHC beam extraction energy. As a future experimental programme, the orbit response will

be measured in detail at 450 GeV/c. At the same time multi-turn acquisitions will be used to determine the phase advance between BPMs as a cross-check.

The experience gained with this program will be used in the future for the LHC transfer lines TI2 and TI8 as well as for the LHC. In particular for the TI8 test in the fall of 2004, results from the trajectory analysis may be available with a short delay of 1-2 hours following the measurements.

Simulations have already shown that for the LHC sector tests, it is already possible to extract information on the LHC main dipole field errors provided the BPM system performance is good [8]. In any case the trajectory response analysis will provide very important information on the BPM and orbit corrector magnets in the LHC.

6 Acknowledgements

The author would like to thank J. Safranek for providing the LOCO code and its documentation.

References

[1] J. Safranek, Nucl. Instr. Meth. **A388** (1997) 27.
J. Safranek *et al.*, *Optics Characterization and Correction at PEP-II*, Proc. of the 1999 Part. Acc. Conf., New York, 1999.

[2] H. Grote and F. Iselin, *The MAD Program*, CERN/SL/90-13 Rev. 5, 1996.

[3] W. Press, B. Flannery, S. Teukolsky and W. Vetterling, *Numerical Recipes*, Cambridge University Press, Cambridge, 1987, 1st ed.

[4] B. Autin and Y. Marti, CERN report ISR MA/73-17, 1973.

[5] J. Wenninger, minutes of the SPS Studies Working Group, 11^{th} June 2002.
J. Wenninger, minutes of the SL Operations Comittee meeting, 4^{th} July 2002.

[6] G. Arduini *et al.*, *2001 SPS Measurements and Modelling of Nonlinear Chromaticity and Detuning with Amplitude at 26 GeV*, SL-Note-2001-049 MD.
J. Wenninger, *Dynamic Effects on Chromaticity for the LHC Beam Cycle in the SPS*, SL-Note-2002-041 OP.

[7] C. Boccard, private communication.

[8] J. Wenninger, *Determination of LHC Main Dipole Field Errors during a Sector Test using Trajectory Analysis*, LHC Project Note 314 (2003).

7 Appendix : Beam Position Monitor Offsets

In LSS5 6 quadrupoles have been equipped with additional windings to allow an individual modulation of the quadrupole strength for optics measurements. The 6 quadrupoles are QD517, QF518, QD519, QF520, QD521 and QF522. Besides the measurement of the local betatron function, the additional windings can also be used to determine the offset between the adjacent BPM and the corresponding quadrupole. For the measurements present herein, the position modulation was observed using the MultiQ acquisition system on the P2 MD cycle at 26 GeV/c. The modulation frequency was 1-2 Hz. The amplitude of the vertical position modulation is shown in Figure 14 as a function of the vertical beam position measured in the adjacent BPM for the 3 QD quadrupoles 517, 519 and 521. The offsets are in the range of 0 to -1.5 mm.

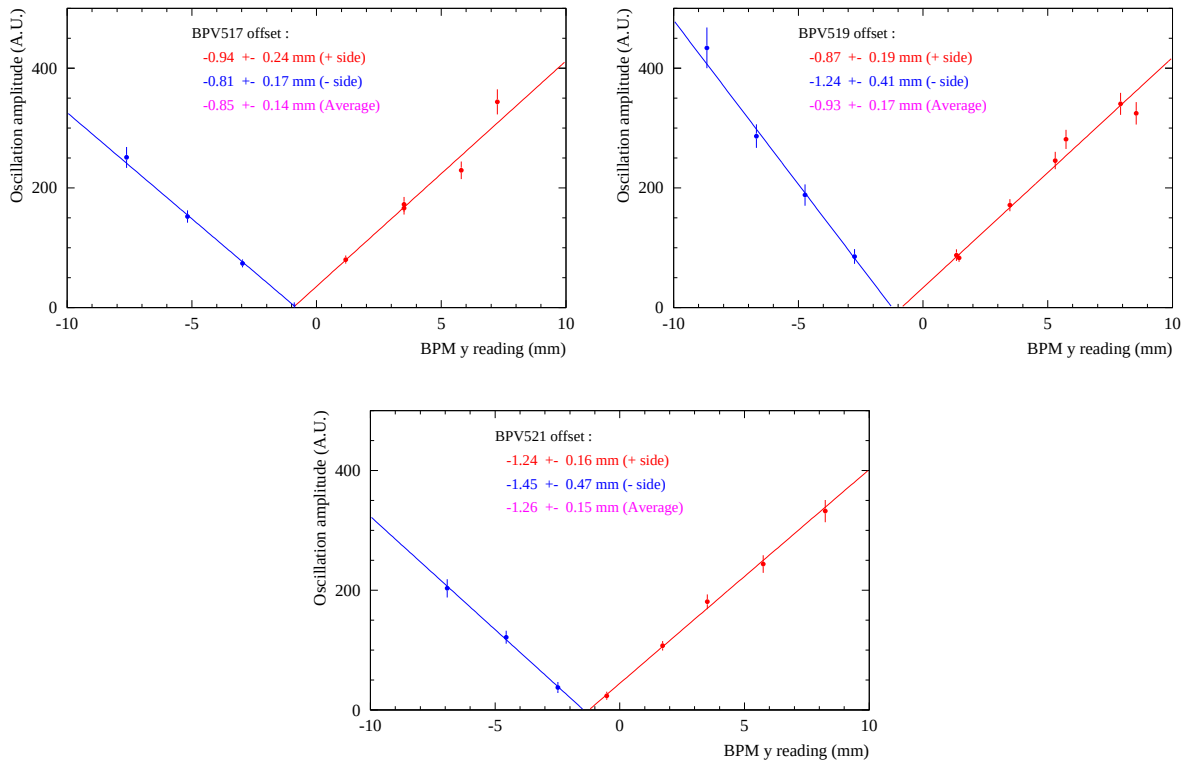

Figure 14: K-modulation measurement results for the 3 vertical BPMs BPV.517, BPV.518 and BPV.521. The amplitude of the position modulation observed on the Q-meter BPM is shown as a function of the beam position determined by the nearby BPV monitor.